Submitted to
Proceedings of the Conference on Design Theory
Edited by Komkov, V.
SIAM : Society for Industrial and Applied Mathematics, Philadelphia, 1991

Generalized Layout Optimization of Three-Dimensional Shell Structures

UM-MEAM-91-07

Katsuyuki Suzuki

and

Noboru Kikuchi*

The University of Michigan
Ann Arbor, MI 48109
United States

February, 1991

* Computational Mechanics Laboratory, Department of Mechanical Engineering and Applied Mechanics, The University of Michigan, Ann Arbor, MI 48109-2215, U.S.A. The authors are supported by DHHS-PHS-G-2-R01-AR34399-04, ONR N-00014-88-K-0637, and NASA Lewis Research Center, NAG 3-1160 during the period when both are working this project.

ensn

UMR6388

Abstract The generalized layout problem involving sizing, shape, and topology optimization is solved by using the homogenization method for three-dimensional linearly elastic shell structures, as an extension of the previous work by Bendsøe and Kikuchi. Formulation, a solution algorithm, several examples of computing the optimum layout of shell structures are presented.

1. Introduction

A modern theory of structural optimization based on mathematical programing and sensitivity analysis is developed by Schmit [1] and Fox [2] in the 60s, although the concept of fully stressed design was widely applied in design practice without solid mathematical justification but with engineers' intuition for a long time. Using variational methods such as Lagrange multipliers and calculus of variations, Prager and Taylor [3] made a justification of the fully stressed design for a class of structural optimization problems by deriving their optimality condition, whose direct use in constructing optimization algorithms leads the so-called optimality criteria method. Structural optimization in the 60s was restricted mostly to sizing problem of frame structures. Even some of topological layout optimization problems of a structure were solved as sizing problems by emphasizing the fact that unnecessary members of frames disappear in the optimization process as the area of the cross section of such members goes to zero. However, these restricted investigation of topology of the optimum structure could not provide significant advancement of the theory of the optimum layout of a structure which enhances the "classical" layout theory of Prager [4] for a very restricted class of structures as an extension of the concept of Michell

* Computational Mechanics Laboratory, Department of Mechanical Engineering and Applied Mechanics, The University of Michigan, Ann Arbor, MI 48109-2215, U.S.A. The authors are supported by DHHS-PHS-G-2-R01-AR34399-04, ONR N-00014-88-K-0637, and NASA Lewis Research Center, NAG 3-1160 during the period when both are working this project.

trusses [5]. Even more recent work by Rozvany [6] in which Prager's idea is extensively developed, deals with layout problems of extremely complex, but still frame structures based on the analytically derived optimality criteria method.

In the present work, we shall extend our scope of layout of a structure, and shall solve layout problems for more general solid structures without assuming frame with complex topology constructed by networking all possible combination of joints distributed in a given design space. In other words, we shall formulate the problem based on the assumption of *continuum* so that any topology of a structure can be generated without assuming any special structural elements and their combination. Furthermore, the shape and size of the optimum structure will also be determined as the result of the design problem without specifying any of parametric representation of the shape and size of a structure. In particular, the optimum layout of three-dimensional shell structures will be studied as an extension of the previous works of the homogenization method introduced in Bendsøe and Kikuchi [7], and also in Suzuki and Kikuchi [8] for plane structures.

2. A Homogenization Method for Plate/Shell Structures

The basic concept of the homogenization method for the generalized layout problem for three-dimensional plate/shell structures is the same to the one for plane elastic structures. Here we shall briefly describe the homogenization method for plate/shell structures. The following is the fundamental steps of the homogenization method of the layout optimization problem :

1) A base shell structure is assumed, the thickness of which is described as a function h_0. This is thickness can be zero, and then we shall consider a complete layout of a structure from the beginning. If h_0 is not zero, a built-up shell structure is assumed with layout of the optimum reinforcement by solving the present optimization problem.

2) A design domain Ω is specified on the curved surface in which the middle surface Ω_0 of the initial shell structure is contained. This domain can be a subset of the middle surface of the initial shell, while it is also possible to be larger than the middle surface.

3) Microscopic perforation is assumed to find the optimum reinforcement of the initial shell by adding solid material whose volume is prescribed. Perforation is characterized by three distributed design variables $\{ a_1, a_2, \theta \}$, the first two are the sizes of the rectangular hole in the unit cell and the angle of rotation of the hole in the macroscopic shell structure. These functions may have different values at different points in the design domain. The "true" size of holes made in the shell structure is really tiny and infinitely many, and they are described by εa_1 and εa_2 for a sufficiently small positive number $\varepsilon>0$. Thus, it may consider there are infinitely many and small rectangular parallelopipes with holes, whose height is a half of a fixed value h_1, on the both sides of the initial shell in order to maintain symmetry of the cross section with respect to the middle surface. A schematic description of the design variables is given in Fig. 1.

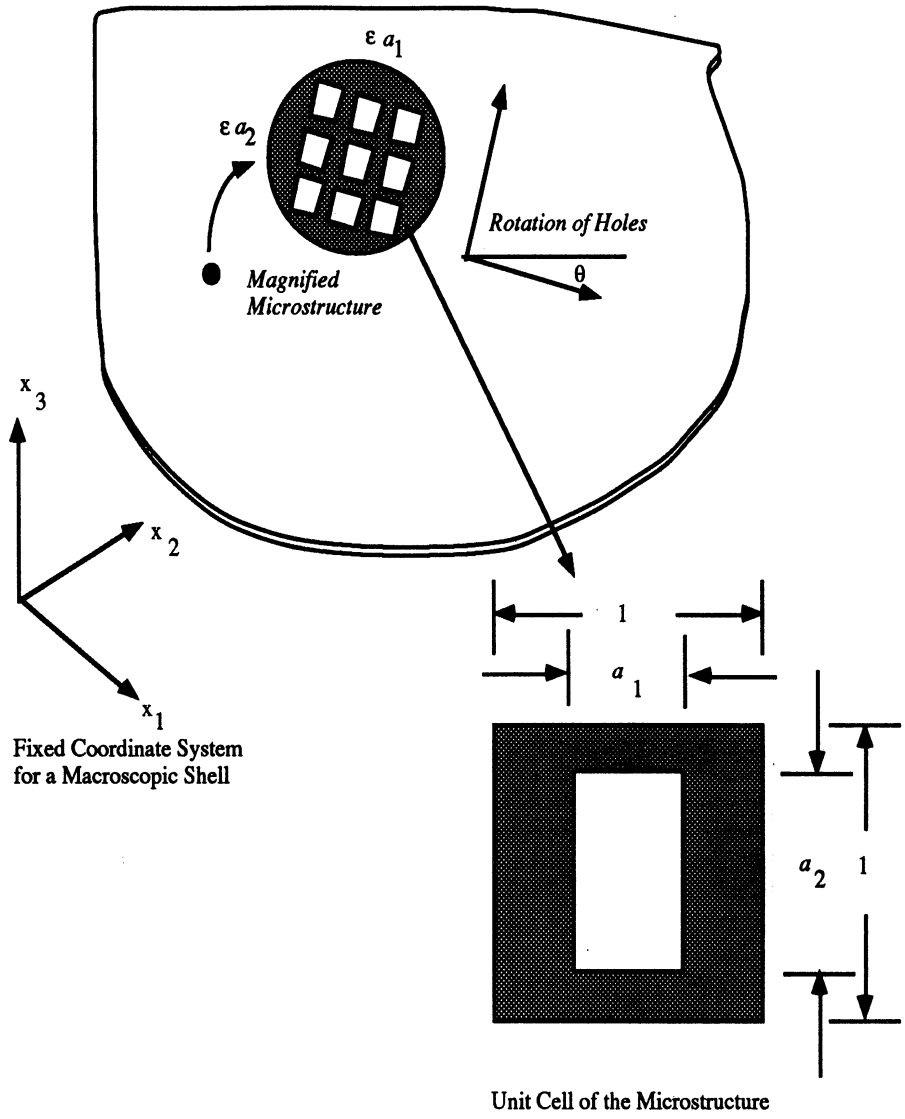

Figure 1 A Schematic Description of the Design Variables on a Three-Dimensional Shell Structure

4) Reinforcement is designed to be constructed by accumulation of appropriate scaling of the unit cell described in Fig. 2 with rotation θ about the normal line to the middle surface. Scaling is taken place only on the middle surface, while the height of the hollow rectangular parallelopipes keeps constant to be a half of h_1 in the both sides of the middle surface. The total volume of reinforcement is given by

$$V_R = \rho h_1 \int_\Omega (1 - a_1 a_2) d\Omega \tag{1}$$

where ρ is the mass density of the material for reinforcement.

5) The optimum design is defined by minimizing the mean compliance of a shell structure for a set of specified loading and support conditions under the volume constraint

$$V_R \leq V_{given} . \tag{2}$$

No other constraints on the stress, strain, and displacement of the shell are assumed in this formulation, while the standard formulation of the optimization is stated as minimizing the total weight of the shell under constraints of the stress, strain, and displacement.

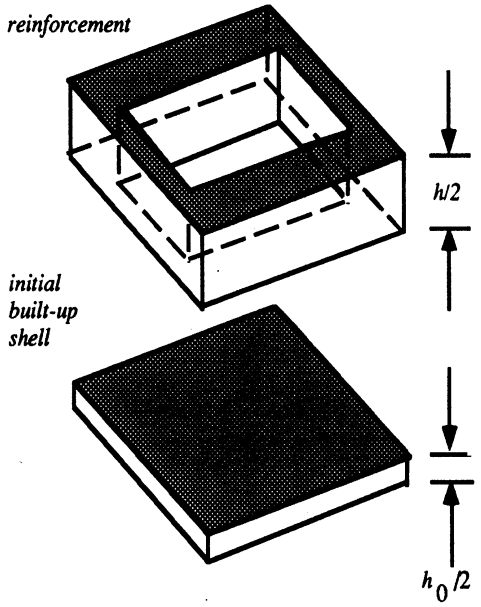

Figure 2 Upper Half Portion of the Unit Cell of the Initial Shell and its Reinforcement

6) To simplify formulation of a shell, let us assume that a curved shell is approximated by union of 4 node quadrilateral finite elements defined by four corner nodes placed in the tree-dimensional space. Further, in order to neglect the curvature effect of a shell, finite element formulation assumes the flat 4 node quadrilateral element obtained by the projection of the original possible non-flat element onto the xy coordinate plane which is defined by minimizing the sum of squares of the distance of corner nodes from the plane. The coordinates x and y are then set up as the principal directions obtained by solving the associated eigenvalue problem. The thickness (i.e. transverse) direction is defined as the normal to the xy plane, and is identified with the z axis. The coordinates (x,y,z) can then define a local coordinate system in which a flat shell element is derived.

Suppose that the displacement field $\{u_x, u_y, u_z\}$ of an arbitrary point P in a shell element Ω_e is approximated by

$$
\begin{aligned}
u_x(x,y,z) &= u(x,y) + z\theta_y(x,y) \\
u_y(x,y,z) &= v(x,y) - z\theta_x(x,y) \\
u_z(x,y,z) &= w(x,y)
\end{aligned} \tag{3}
$$

where $\{u, v, w\}$ is the displacement field of the point P' of the projection of P on the middle surface of the shell that coincides with the xy plane, θ_x and θ_y are the rotation of P about the x and y axes, respectively. This approximation of the displacement field yields the strains :

$$
\begin{aligned}
\{\varepsilon\}^T &= \left\{\varepsilon_x \;\; \varepsilon_y \;\; \varepsilon_y \;\; \gamma_{yz} \;\; \gamma_{zx} \;\; \gamma_{xy}\right\} \\
&= \left\{\frac{\partial u_x}{\partial x} \;\; \frac{\partial u_y}{\partial y} \;\; \frac{\partial u_z}{\partial z} \;\; \frac{\partial u_y}{\partial z} + \frac{\partial u_z}{\partial y} \;\; \frac{\partial u_z}{\partial x} + \frac{\partial u_x}{\partial z} \;\; \frac{\partial u_x}{\partial y} + \frac{\partial u_y}{\partial x}\right\} \\
&= \left\{\frac{\partial u}{\partial x} \;\; \frac{\partial v}{\partial y} \;\; 0 \;\; 0 \;\; 0 \;\; \frac{\partial u}{\partial y} + \frac{\partial v}{\partial x}\right\} \\
&+ z\left\{\frac{\partial \theta_y}{\partial x} \;\; -\frac{\partial \theta_x}{\partial y} \;\; 0 \;\; 0 \;\; 0 \;\; \frac{\partial \theta_y}{\partial y} - \frac{\partial \theta_x}{\partial x}\right\} \\
&+ \left\{0 \;\; 0 \;\; 0 \;\; -\theta_x + \frac{\partial w}{\partial y} \;\; \frac{\partial w}{\partial x} + \theta_y \;\; 0\right\}
\end{aligned} \tag{4}
$$

Using the contracted notation, the internal virtual work in an arbitrary shell element Ω_e can be written by

$$
\delta U_e = \int_{\Omega_e} \int_{-h_1/2}^{h_1/2} \{\delta\varepsilon\}^T [D] \{\varepsilon\} dz d\Omega \tag{5}
$$

where $[D]$ is the elasticity matrix in the contracted notation obtained by assuming the plane stress condition in the xy plane. The matrix $[D]$ is defined by the elasticity tensor $\mathbb{E}^G$ obtained by rotation θ of the homogenized elasticity tensor $\mathbb{E}^H$ for plane stress problems. Applying the symmetry condition with respect to the middle surface, the internal virtual work in Ω_e can be written by

$$
\begin{aligned}
\delta U_e = &\int_{\Omega_e} \left(\{\delta\varepsilon_m\}^T [D_0] \{\varepsilon_m\} + \{\delta\kappa_B\}^T [D_2] \{\kappa_B\} + \{\delta\gamma\}^T [D_{ts}] \{\gamma\} \right) d\Omega \\
&+ \bar{\alpha}^2 \delta\theta_z \theta_z
\end{aligned} \tag{6}
$$

where

$$
[D_0] = \int_{-h_1/2}^{-h_0/2} \left[D_m(a_i,\theta)\right] dz + \int_{-h_0/2}^{h_0/2} \left[D_m(0,0)\right] dz + \int_{h_0/2}^{h_1/2} \left[D_m(a_i,\theta)\right] dz
$$

$$
[D_2] = \int_{-h_1/2}^{-h_0/2} \left[D_m(a_i,\theta)\right] z^2 dz + \int_{-h_0/2}^{h_0/2} \left[D_m(0,0)\right] z^2 dz + \int_{h_0/2}^{h_1/2} \left[D_m(a_i,\theta)\right] z^2 dz
$$

$$[D_{ts}]=\int_{-h_1/2}^{-h_0/2}[D_s(a_i,\theta)]dz+\int_{-h_0/2}^{h_0/2}[D_s(0,0)]dz+\int_{h_0/2}^{h_1/2}[D_s(a_i,\theta)]dz$$

$$[D_m(a_i,\theta)]=\begin{bmatrix} D_{11}(a_i,\theta) & D_{12}(a_i,\theta) & D_{16}(a_i,\theta) \\ & D_{22}(a_i,\theta) & D_{26}(a_i,\theta) \\ SYM & & D_{66}(a_i,\theta) \end{bmatrix} \qquad [D_s]=\beta\begin{bmatrix} D_{44} & 0 \\ 0 & D_{55} \end{bmatrix}$$

$$\{\varepsilon_m\}=\begin{Bmatrix} \partial u/\partial x \\ \partial v/\partial y \\ \partial u/\partial y+\partial v/\partial x \end{Bmatrix} \qquad \{\kappa_B\}=\begin{Bmatrix} -\partial\theta_y/\partial x \\ \partial\theta_x/\partial y \\ \partial\theta_x/\partial x-\partial\theta_y/\partial y \end{Bmatrix} \qquad \{\gamma\}=\begin{Bmatrix} -\theta_x+\partial w/\partial y \\ \theta_y+\partial w/\partial x \end{Bmatrix}$$

and

$$\overline{\alpha}^2=\alpha^2 h_1\int_{\Omega_e}\{(x-x_0)^2D_{44}+(y-y_0)^2D_{55}\}d\Omega_e$$

Here (x_0, y_0) may be identified with the centroid of Ω_e, α is a very small number, and β is the so-called shear correction factor. α_i are sizes and θ is angle of rotation of microscopic holes that only exists in $[-h_1/2,-h_0/2]$ and $[h_0/2,h_1/2]$. As shown in above the design variables $\{ a_1, a_2, \theta \}$ define the D matrices in the shell formulation, and thus, for a set of their fixed values we can regard the above a standard shell formulation that can be found in the literature of finite element analysis of shells, see, e.g., Noor, Belytschko, and Simo[9]. Since "torsional" rigidity is introduced artificially, this model involves 5 degrees of freedom per node. It is also noted that the homogenization process is applied at the level of the D matrix before integrating it in the thickness direction to compute appropriate rigidity for a plate/shell.

Approximating u, v, w, θ_x, and θ_y by bilinear polynomials in the parametric coordinates ξ and η, using the shape functions

$$N_\alpha(\xi,\eta)=\frac{1}{4}(1+\xi_\alpha\xi)(1+\eta_\alpha\eta) \qquad \alpha=1,\ldots,4 \tag{7}$$

where $\{(\xi_\alpha, \eta_\beta)\}$ are the parametric coordinates of the four corner nodes of an element. Applying this approximation, we discretize the total strain energy, and then the internal virtual work of the shell is approximated. Indeed, in each finite element we obtain the element stiffness matrix in the local coordinate system (x,y,z) :

$$[K_e]=\int_{\Omega_e}[B_m]^T[D_0][B_m]d\Omega+\int_{\Omega_e}[B_B]^T[D_2][B_B]d\Omega$$
$$+\int_{\Omega_e}[B_\gamma]^T[D_{ts}][B_\gamma]d\Omega+[k_\alpha]^T[k_\alpha] \tag{8}$$

Here

$$\{\varepsilon_m\} = \sum_{\alpha=1}^{4} \begin{bmatrix} \frac{\partial N_a}{\partial x} & 0 & 0 & 0 & 0 & 0 \\ 0 & \frac{\partial N_a}{\partial y} & 0 & 0 & 0 & 0 \\ \frac{\partial N_a}{\partial y} & \frac{\partial N_a}{\partial x} & 0 & 0 & 0 & 0 \end{bmatrix} \begin{Bmatrix} u_\alpha \\ v_\alpha \\ w_\alpha \\ \theta_{x\alpha} \\ \theta_{y\alpha} \\ \theta_{z\alpha} \end{Bmatrix} = [B_m]\{d_e\}$$

$$\{\kappa_B\} = \sum_{\alpha=1}^{4} \begin{bmatrix} 0 & 0 & 0 & 0 & -\frac{\partial N_a}{\partial x} & 0 \\ 0 & 0 & 0 & \frac{\partial N_a}{\partial y} & 0 & 0 \\ 0 & 0 & 0 & \frac{\partial N_a}{\partial x} & -\frac{\partial N_a}{\partial y} & 0 \end{bmatrix} \begin{Bmatrix} u_\alpha \\ v_\alpha \\ w_\alpha \\ \theta_{x\alpha} \\ \theta_{y\alpha} \\ \theta_{z\alpha} \end{Bmatrix} = [B_B]\{d_e\}$$

$$\{\gamma\} = \sum_{\alpha=1}^{4} \begin{bmatrix} 0 & 0 & \frac{\partial N_\alpha}{\partial y} & -N_\alpha & 0 & 0 \\ 0 & 0 & \frac{\partial N_\alpha}{\partial x} & 0 & N_\alpha & 0 \end{bmatrix} \begin{Bmatrix} u_\alpha \\ v_\alpha \\ w_\alpha \\ \theta_{x\alpha} \\ \theta_{y\alpha} \\ \theta_{z\alpha} \end{Bmatrix} = [B_\gamma]\{d_e\}$$

$$\theta_z = \sum_{\alpha=1}^{4} \{0 \quad 0 \quad 0 \quad 0 \quad 0 \quad \overline{\alpha}/4\} \begin{Bmatrix} u_\alpha \\ v_\alpha \\ w_\alpha \\ \theta_{x\alpha} \\ \theta_{y\alpha} \\ \theta_{z\alpha} \end{Bmatrix} = [k_\alpha]\{d_e\}$$

$$\delta U_e = \{\delta d_e\}^T [K_e]\{d_e\}$$

and $\{d_e\}$ is the vector of the degrees of freedom in an element. Applying appropriate numerical integration rules which yield equivalent effect of appropriately assumed stress or strain fields in an element, we can compute the element stiffness matrix of the shell. Details of such integration schemes can be found in Noor, Belytschko, and Simo[9].

7) If the shell is subject to external forces and moments on the lateral surfaces and its boundary, we can derive an approximation using the 4 node quadrilateral element. We shall represent such an approximation by

$$\delta P_e = \{\delta d_e\}^T \{f_e\} \tag{9}$$

where δP_e is the work done by the external forces and moment of an element Ω_e, and $\{ f_e \}$ is the set of equivalent nodal forces and moments with respect to the degrees of freedom in a finite element.

Thus, the total potential energy of the shell structure is approximated by the discrete form

$$\Pi(\{d_e\}) = \sum_{e=1}^{E} \frac{1}{2}\{d_e\}^T [K_e]\{d_e\} - \{d_e\}^T \{f_e\} \tag{10}$$

where E is the number of finite elements covering the shell structure, i.e., design domain in the optimum reinforcement problem. It is clear that the element stiffness matrix $[K_e]$ depends on the design variables $\{ a_1, a_2, \theta \}$.

8) Since the design problem is defined by minimizing the mean compliance under the volume constraint for the amount of reinforcement material, its finite element approximation is given as follows :

$$\underset{V_R = \rho h_1 \int_\Omega (1 - a_1 a_2) d\Omega \le V_{given}}{Minimize} \quad \sum_{e=1}^{E} \{d_e\}^T \{f_e\} \tag{11}$$

Noting that

$$\Pi(\{d_e\}) = -\sum_{e=1}^{E} \frac{1}{2}\{d_e\}^T \{f_e\} = \underset{\{\bar{d}_e\}}{Minimize} \ \Pi(\{\bar{d}_e\})$$

we can define the optimization problem by

$$\underset{V_R = \rho h_1 \int_\Omega (1 - a_1 a_2) d\Omega \le V_{given}}{Minimize} \quad \left(-2 \underset{\{\bar{d}_e\}}{Minimize} \ \Pi(\{\bar{d}_e\}) \right) \tag{12}$$

Introducing the Lagrange multiplier $\lambda \le 0$ to the volume constraint, and defining the Lagrangian

$$L = \Pi - \lambda \left(\rho h_1 \sum_{e=1}^{E} \int_{\Omega_e} (1 - a_1 a_2) d\Omega - V_{given} \right), \tag{13}$$

the first variation of this Lagragian with respect to the design variables, degrees of freedom in the finite element model, and the Lagrange multiplier, yields the optimality condition of the finite element approximation of the design problem :

$$\sum_{e=1}^{E}[K_e]\{d_e\}=\sum_{e=1}^{E}\{f_e\}$$

$$\frac{1}{2}\{d_e\}^T\left(\frac{\partial}{\partial a_1}[K_e]\right)\{d_e\}+\lambda\rho h_1 a_2=0$$

$$\frac{1}{2}\{d_e\}^T\left(\frac{\partial}{\partial a_2}[K_e]\right)\{d_e\}+\lambda\rho h_1 a_1=0 \qquad e=1,....,E$$

$$\frac{1}{2}\{d_e\}^T\left(\frac{\partial}{\partial \theta}[K_e]\right)\{d_e\}=0$$

$$\lambda\left(\rho h_1\sum_{e=1}^{E}\int_{\Omega_e}(1-a_1a_2)d\Omega-V_{given}\right)=0 \qquad (14)$$

Applying the optimality criteria method described in Bendsøe and Kikuchi [7] and also in Suzuki and Kikuchi [8], we can derive a computational scheme to determine the design variables { a_1, a_2, θ }. In the present work, we discretize the design variables by piecewise constant functions, i.e., within a finite element , a_1 , a_2 , and θ are assumed to be constant. Thus 3E discrete design variables are introduced in the discrete optimization problem.

9) It is noted that the height h_1 of the microscopic hollow rectangular parallelopipes is assumed to be constant in the optimization problem, while the sizes of hollowness, a_1 and a_2, are assumed to vary in design. The standard treatment of the optimum reinforcement of a plate/shell structure is defined by obtaining the thickness of added reinforcement to the initial thin plate/shell structure. In other words, the design variable is the thickness $h_1(x,y)$ of the reinforcement. In the present approach, we assume the constant height of the "ribs," but their sizes and the orientation will be determined so as to the optimization is achieved, and also the existence of microscopic ribs is expected, although they may not be formed as the result of the optimization. The present optimization can be classified as a sizing optimization problem, but the choice of the sizes to be optimized is non-standard.

Another characteristics of the present approach is that the homogenization process is applied at the level of the D matrix of a solid, instead of applying the homogenization to the bending rigidity. If there are infinitely small stiffeners in the perpendicular direction of the x axis as shown in Fig. 3, the present approach does not alter the bending rigidity of the initial plate/shell in the x direction at all, since the homogenized elasticity constant in the x direction of the unidirectional stiffened panel is the same to the one without stiffeners. However, if the homogenization process is taken for the bending rigidity, this unidirectional stiffeners may contribute to increase of the overall bending rigidity if the height of stiffeners is sufficiently high. Thus, the present approach cannot produce unidirectional discrete stiffeners to increase the bending rigidity, despite of its capability of significant increase by their use. In other wards, despite of possibility of the existence of fine microstructures in the present formulation, we *prevent* the existence of unidirectional discrete stiffeners, and then the

optimum layout computed by the present formulation can be *suboptimum* to the one obtained by the formulation that the homogenization process is applied at the level of bending rigidity, see Bendsøe [10], since it can produce unidirectional discrete stiffeners. In this sense, the present formulation does possess limitation to produce the optimum, but it can be still useful in practice of structural design optimization in which distribution of infinitely many and microscopic discrete stiffeners is unrealistic in manufacturing. Most of engineering applications prefer not to have infinitely many microscopic discrete stiffeners, but they place a finite number of macroscopic discrete stiffeners. The present formulation can provide such solutions, rather than *the* optimum that involves infinitely many discrete stiffeners.

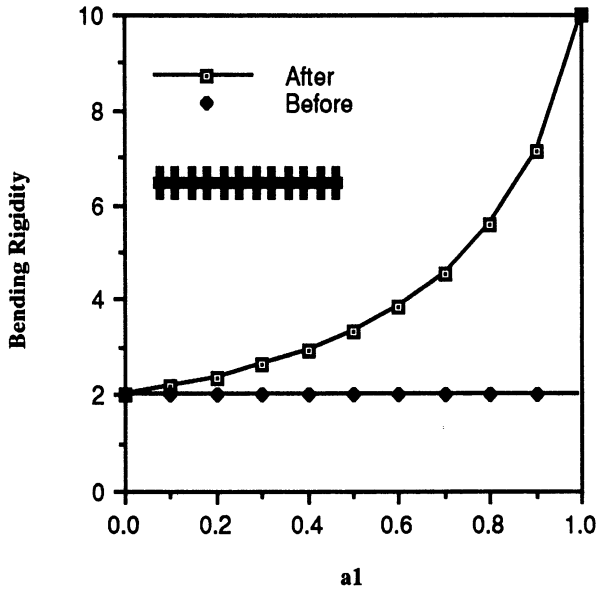

Figure 3 Homogenized Bending Rigidity of a Unidirectionally Stiffened Beam
(after : Bending rigidity is homogenized)
(before : D matrix is homogenized)

Since nonlinearity of the bending rigidity of the plate/shell computed by the present approach is much stronger than the case that bending rigidity is homogenized, convergence of an iteration scheme by the optimality criteria method for optimization may not be smooth. In other words, some special care may be necessary to deal with this strong nonlinearity with respect to the design variables a_1 and a_2.

10) Thickness optimization of a plate/shell structure has been extensively studied in structural optimization by, e.g., Schmit et al. [11], Morrow and Schmit [12], Simitses [13], Banichuk [14], Haftka and Prasad [15], Cheng [16], Cheng and Olhoff [17,18], and others. Especially, majority of literature related to this subject can be found in the survey paper Haftka and Prasad [15] and a general theory of the thickness optimization of a plate can be found in Banichuk[14] for the case that the variation of the thickness is sufficiently smooth so that discrete stiffeners should not appear in the optimum. Delicate discussion on convergence and mechanical models of a plate/shell is discussed in Cheng [16], as well as importance of introduction of the homogenization method is demonstrated in Cheng and Olhoff [17,18] and also in Bendsøe [10]. A layout theory of plates are also discussed in Rozvany[19] with a different context from the present approach.

3. Optimum Layout of Beam and Arch Structures

We shall first study layout problem of a beam/arch structure using the above formulation before extending the homogenization method to a three-dimensional plate/shell structure. To this end, a beam/arch is regarded as a two-dimensional plane structure.

The first example is a layout problem shown in Fig.4 that can be found in standard textbooks on structural optimization. If this problem is regarded as a sizing problem that finds the optimal thickness of the rectangular cross section of a beam with a fixed width, this problem can be solved easily by applying a standard technique of structural optimization.

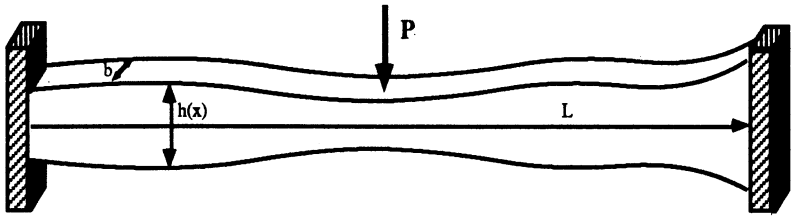

Figure 4 Thickness optimization problem of clamped beam

The problem of minimizing mean compliance subject to equilibrium equation and volume constraint is equivalent to

$$\max_{h} \min_{w} \left\{ \int_0^L \frac{1}{2} Ebh^3 \left(\frac{d^2w}{dx^2} \right)^2 dx - Pw\big|_{x=L/2} \right\} \tag{15}$$

subject to

$$\int_0^L bh\,dx - V \le 0 \tag{16}$$

Here w is vertical displacement, h is height of beam that is to be designed, and b is width of beam that is fixed, E is Young's modulus, P is applied point load, and V is upper bound on volume. Using Lagrange multiplier method, necessary condition for optimum can be derived as

$$h^2 \left(\frac{d^2w}{dx^2} \right)^2 = \text{constant} \quad (0 \le x \le L) \tag{17}$$

From boundary conditions, the analytical answer for optimal distribution of thickness becomes

$$h(x) = \frac{3\bar{V}}{2bL}\sqrt{\left|1-\frac{x}{(L/4)}\right|} \qquad (0 \le x \le L/2) \tag{18}$$

and symmetric when $L/2 < x < L$. The answer is shown in Fig. 5.

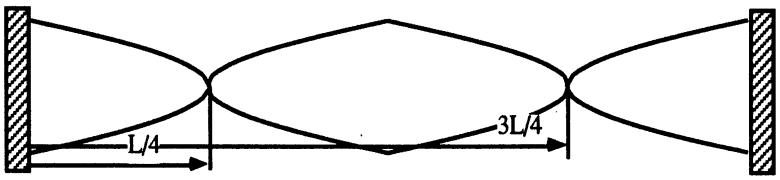

Figure 5. Analytical solution of beam thickness design

The optimal thickness distribution yields two hinges at $x=L/4$ and $3L/4$, i.e., $h = 0$ at $x=L/4$ and $3L/4$, while the maximum thickness is obtained at x=0, $L/2$, and L. The gradient h' of the thickness is ∞ at a=$L/4$ and $3L/4$.

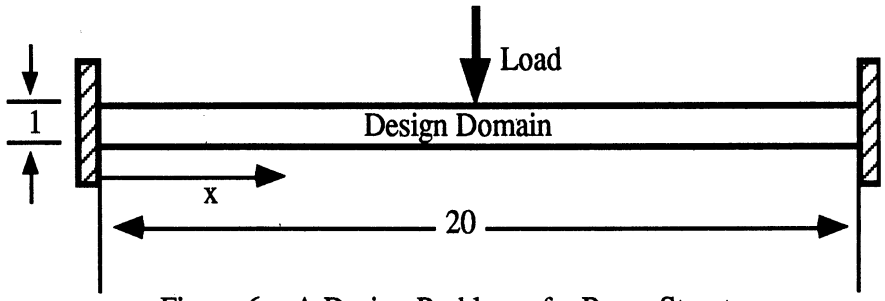

Figure 6. A Design Problem of a Beam Structure

Now let us solve a similar problem using the homogenization method based on the formulation given in the previous section. To do this, we shall consider the optimum layout problem in a very narrow strip shown in Fig. 6. A shear force is applied along the center of the narrow strip and this force is transmitted to the fixed supports in both sides by a structure constructed. Dividing the narrow design domain into 200 x 10 uniform size 4 node finite elements, we shall solve the discrete optimization problem (12) to determine the optimum layout for three different volumes of "reinforcement." Note that in this example, we assume that $h_0 = 0$, i.e., there is no initial plate structure assumed. The total number of discrete design variables is 6,000, while the total number of the degrees of freedom of the finite element model of the design domain is 4,422 since plane stress condition is assumed without any of transverse deformation. Computed results are shown in Fig.7. It is clear that hinges appear at x=5 and 15, same way as beam solution goes. Since it is possible to generate internal holes inside the optimal structure, holes are naturally formed to increase the stiffness against bending moment. i.e. forms sandwich beam. In most of thickness optimization studies published so far, internal holes are not presented. Thus, the method introduced in this paper can provide far more sophisticated optimal structure. If the volume of solid material is reduced, very truss like structures are formed. Because of the restriction on the design domain, reinforcement can be placed only inside the very narrow rectangular domain. Large reinforcement is observed in the vicinity of the fixed end points as well as the center at which the point force is applied. It is clear that the present method can provide the shape and topology of the overall

structure as well as the optimal sizes of members of a "truss" structure, and that there have been no other methods which have comparable capability to the present one.

Volume Constraint 10

Volume Constraint 15

Volume Constraint 18

Figure 7. Optimal Layout of a Beam like Structure

As shown in Fig. 7, hinges appear in the optimal structure if a beam like structure is assumed. Now let us solve the similar problem for an arch which can take both inplane and transverse forces.(Fig. 8) Because of curvature, large portion of the transverse force applied at the center is transferred as axial force along the axis of an arch. Thus, formation of hinges is unrealistic in such a structure, i.e., the optimal layout for an arch like structure should be very different from the one for a beam. Indeed, Figure 9 shows the optimal layout for three different volumes of solid material. No hinges are generated. Furthermore, the present method can find the best layout of the axis of an arch as well as the thickness. To do this, a standard method requires sensitivity analysis of the position of the axis of an arch as well as the thickness distribution. In the present method, it is not necessary to provide these information. The optimal configuration of an arch is automatically obtained without specifying its function forms.

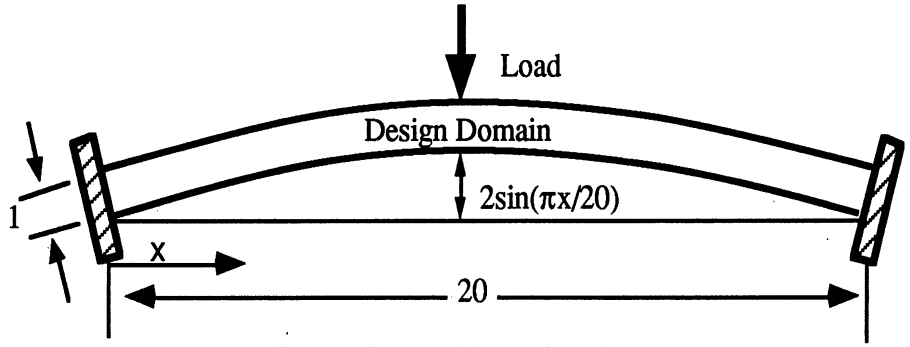

Figure 8. Design Problem of Arch structure

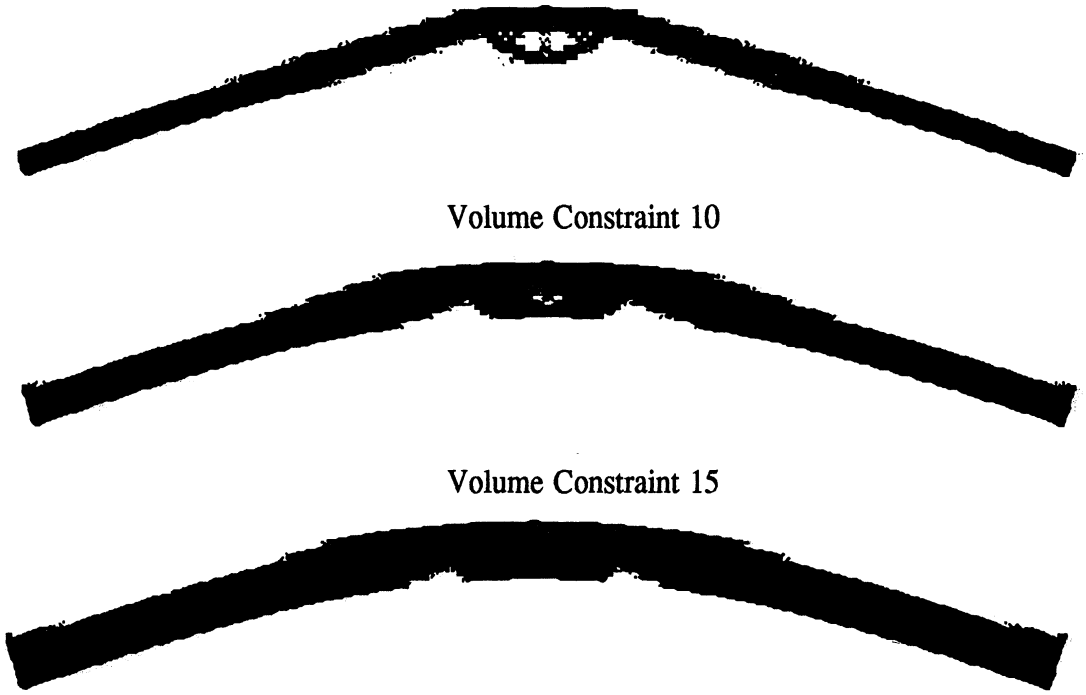

Volume Constraint 10

Volume Constraint 15

Volume Constraint 18

Figure 9. Optimal Layout of an Arch Structure

4. Optimum Layout of a Simply Supported Plate

For demonstration of the homogenization method to find the optimal layout of a plate/shell structure, we shall consider a simply supported plate subject to two loading cases : a concentrated force at the center and uniformly distributed pressure on the plate. The size of the plate is 60 cm × 60 cm as shown in Figs. 10 and 11. Using symmetry of the geometry and the loading condition considered here, one quarter of the domain need be modeled by 4 node finite elements to find the optimal layout of reinforcement of a thin plate of the initial thickness h_0=0.1cm. The height of "stiffeners" which are introduced for reinforcement is restricted to h_1=1cm. A quarter of the plate, i.e. the design domain is divided into 30x30 square and uniform finite elements in which 2,700 discrete design variables are involves while the total number of degrees of freedom of the finite element model is 4,805 because of 5 degrees of freedom per node. Young's modulus of the reinforcement and the initial plate material is assumed to be 200 GPa, while Poisson's ratio is 0.29. We shall apply two different loads, a point transverse force at the center and a uniformly distributed transverse load on the plate.

The optimal distribution of reinforcement of a thin plate is obtained as shown in Fig. 12 for the point load. If the volume of reinforcement (i.e. solid material added to the original thin plate) is very large, no reinforcement are assigned in the vicinity of the lines connected for the mid-points of two adjacent boundary edges of the plate. A square plate rotated 45 degree is formed as a part of stiffeners. If the thickness of the middle thin plate is assumed to be zero, i.e., h_0=0, the optimal layout of solid material to form a plate structure must yield line hinges along these four 45 degree inclined lines. It is reminded that two hinges are generated for a beam when its thickness is

optimized for the case of point load at the center of the clamped beam, see Section 3. Thus, line hinges in the optimal reinforcement may be expected. It should be noted that this does not mean discontinuity of the transverse displacement along these hinge lines.

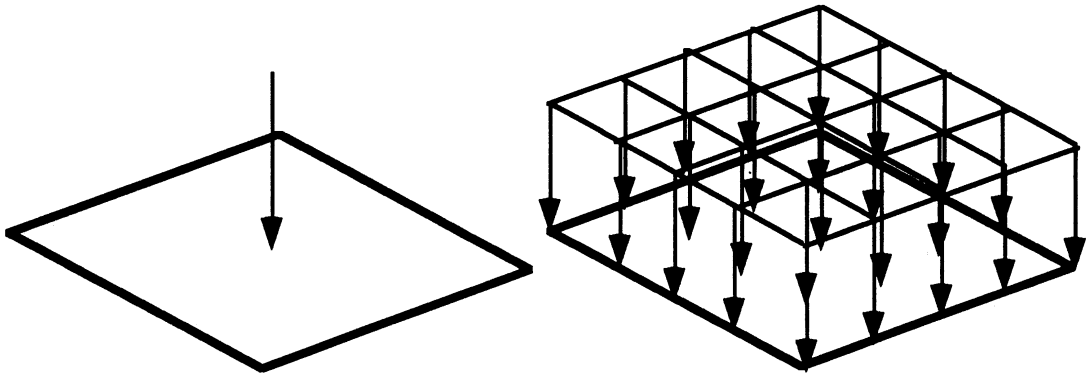

Figure 10 Simply Supported Square Plate Subject to Two Different Loading Conditions

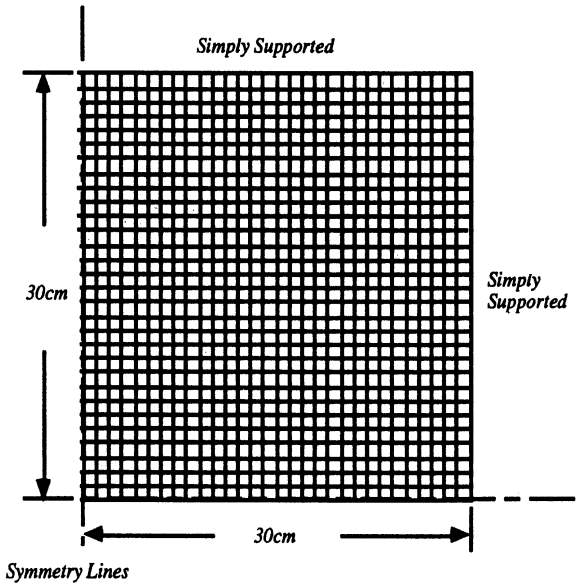

Figure 11 Finite Element Model of a Quarter Portion of the Plate

But only the slope may be discontinuous, and it is still admissible in the variational formulation of an elastic plate defined in the Sobolev space $H^2(\Omega)$. The slope, i.e., the normal derivative of the transverse deflection w along a finite number of curves in the plate can be discontinuous. In this sense, the optimal reinforcement or layout pushes the transverse deflection w to the limit of the admissible space, in other words, w is just in $H^2(\Omega)$ but not in $H^{2+\delta}(\Omega)$ for $\delta>0$. This, further, may imply that proof of convergence of finite element approximations requires very delicate argument when the representative mesh size goes to zero, since it expects extra regularity (smoothness) of the solution to obtain the rate of convergence of the finite element approximation. It should be possible to establish strong convergence of the finite element approximations to the optimal solution, but it may be difficult to establish an explicit rate of convergence.

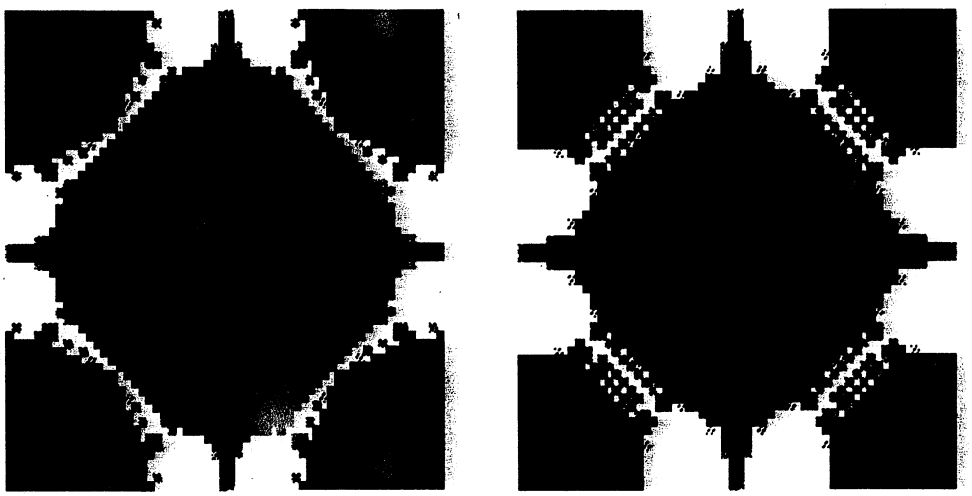

(a) volume 720/900 (b) volume 630/900

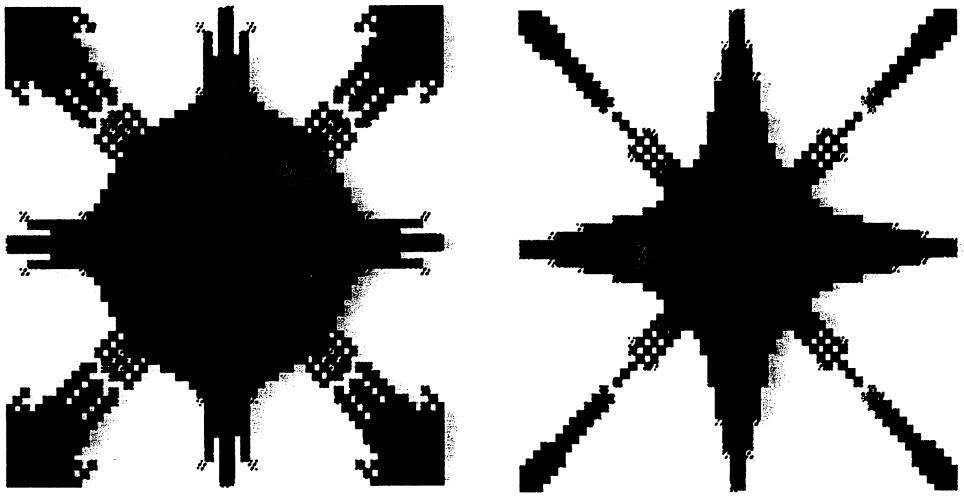

(c) volume 450/900 (d) volume 270/900

Figure 12 Optimal Layout of reinforcement of a Plate with Point Load

To explain the result obtained in Fig.12 for the optimum layout of reinforcement, let us introduce a fact of limit line analysis of plasticity in which slip lines appear, see Figure 13. It can be easily understood that the reinforcement in layout optimization are formed on the slip lines of limit analysis obtained in Yang[20]. Here, because of formation of four hinge lines in the optimum layout, these behaves so as to the simply supported boundary, and then two more slip lines are added by connecting diagonals of this "newly" formed simply supported plate. Most of reinforcement is formed along the slip lines, and this seems to be a natural consequence. When limit lines appears, displacement becomes infinite in linear theory, while our objective of reinforcement is to minimize the mean compliance which yields the minimum displacement for a specified load. To avoid plastic hinges in limit analysis, reinforcement in an elastic plate must be along these lines. A rather thick cross shape stiffener on the center (which corresponds to slip lines of the inner simply supported plate generated by appearance of four hinges in the reinforcement) and thin stiffeners along the diagonals of the original plate, are formed. Note that the black portion in the figures indicates

that no holes are generated over there in reinforcement i.e. stiffeners or plates whose height is fixed to be h_1-h_0. Another interesting observation is that solid stiffeners or plates are generated in most of the portion. There is very little perforation in the optimal design, although it is allowed. In other words, fine microstructure by perforation may not be the optimum as far as the present result is concerned.

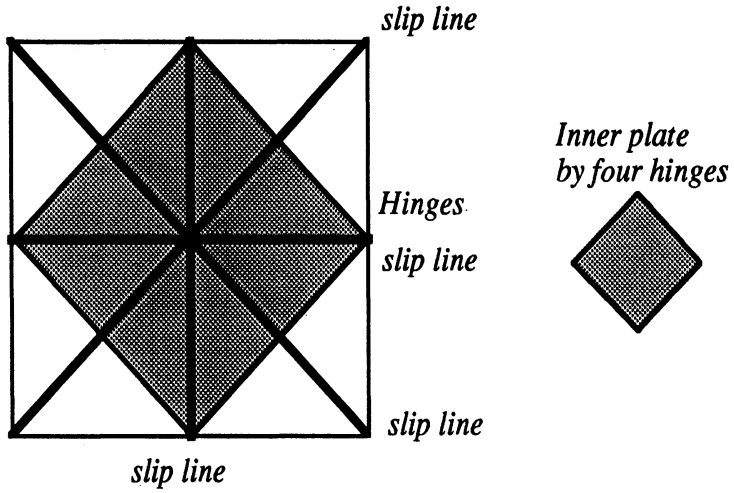

Figure 13 Slip Lines of Simply Supported Plates in Limit Analysis

Figure 14 shows the result for a plate with the uniformly distributed load. It is noteworthy that in the distributed load case, additional stiffeners appear in the four corner area. The overall layout for this case is the same to the one for the point load.

(a) volume 450/900 (b) volume 270/900

Figure 14 Optimal Layout of a Plate with Distributed Load

Another interesting question is whether the present homogenization method is stable in finite element element approximations. That is, when the finite element model of a three-dimensional shell structure is refined systematically, it is important to know whether the displacement of the shell and the optimum layout of reinforcement do converge to the unique solutions. In this case, the height h_1 of the

stiffener which is characterized by the microstructure of the hollow rectangular parallelopipe is assumed to be constant, while the thickness of the initial shell h_0 is also fixed to be a sufficiently small number. Similar convergence of finite element approximations is considered for plane structures in the previous paper [8]. We shall examine convergence of the finite element approximation by using the layout optimization of the plate with a concentrated force applied at the center of the plate. To do this, a quarter portion of the square plate is divided into three different meshes: 20x20, 30x30, and 40x40 uniform square 4 node finite elements for the volume of reinforcement 720 while the total area of design domain is 900. The optimum layouts of reinforcement are obtained as shown in Fig. 15, and it is clear that the configuration of the optimum layout is unchanged by finite element mesh refinement except very details of reinforcement. In other words, convergence of the finite element approximation can be expected for the present formulation. The value of the mean compliance of the optimum structure is also affected by the finite element refinement in ver small amount, i.e., convergence is attained. As refinement is taken place, very fine details of reinforcement can be observed, although the overall layout is unchanged.

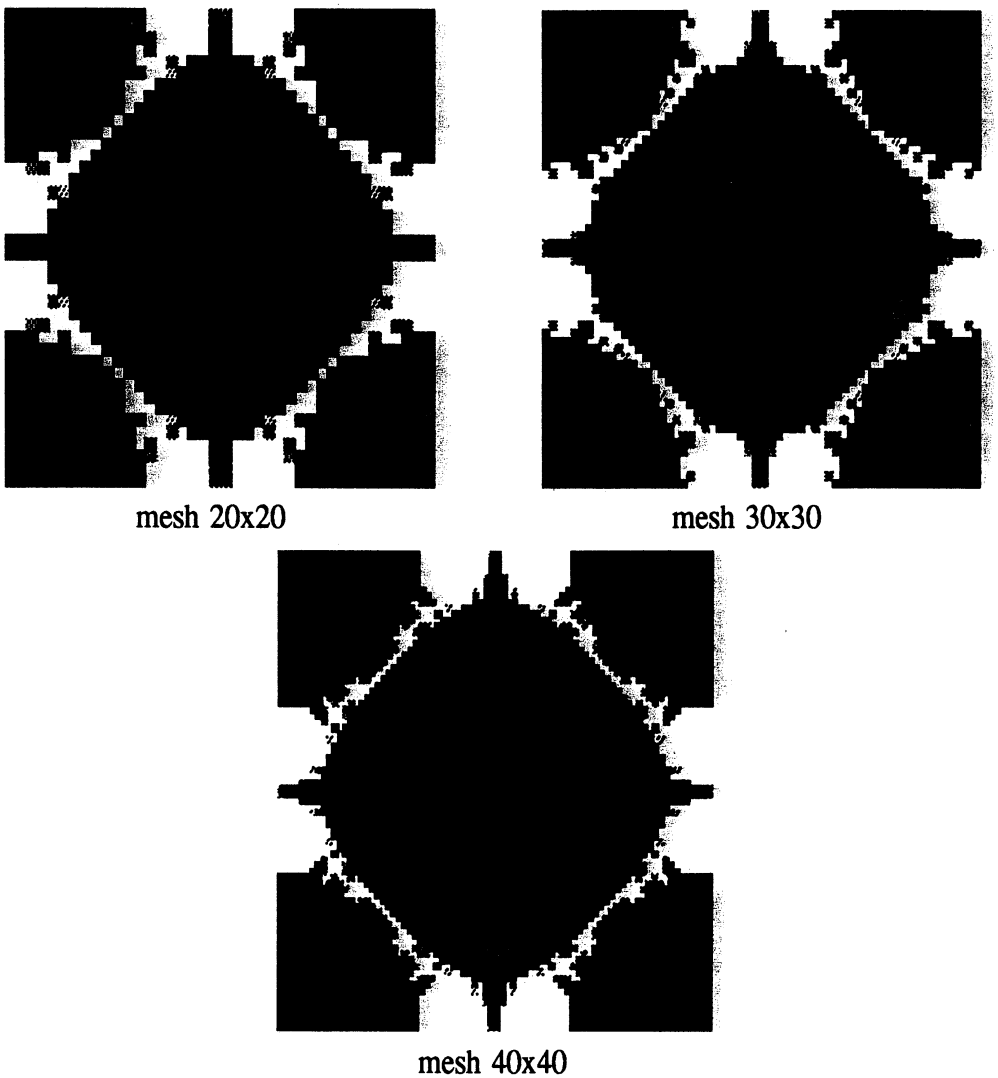

Figure 15 Convergence of the Finite Element Approximation

5. Optimum Layout of a Simply Supported Shallow Shell

Let us consider a shallow shell whose projected plane to the xy plane is the same to the plate considered in the previous section. The shallow shell is defined by the curved surface

$$z(x,y) = z_{\max} \sin \pi \frac{x}{x_{\max}} \sin \pi \frac{y}{y_{\max}} \qquad \textit{where} \qquad \frac{z_{\max}}{x_{\max}} = \frac{z_{\max}}{y_{\max}} = \frac{1}{12}.$$

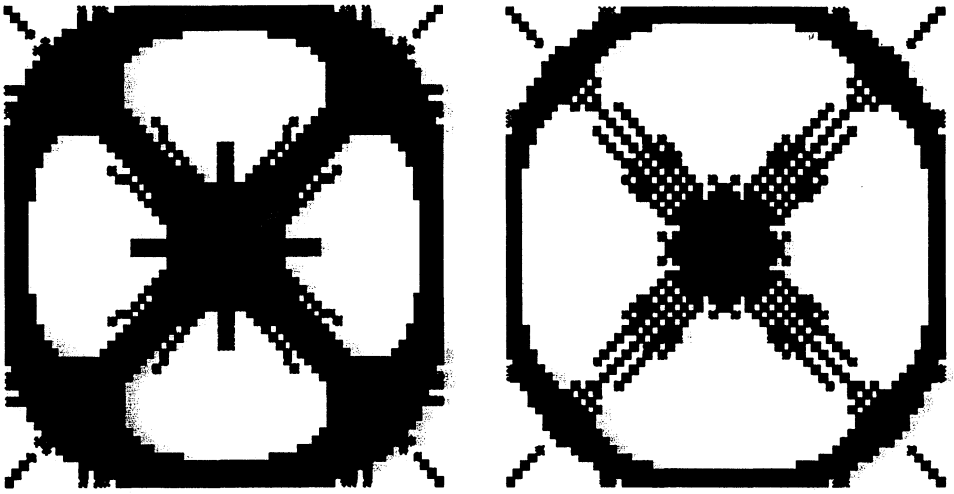

(a) volume 450/900 (b) volume 270/900

Figure 16 Shallow Shell with the Point Load at the Center

(a) volume 450/900 (b) volume 270/900

Figure 17 Shallow Shell with the Uniformly Distributed Load

The results of a shell are very different from those of a plate as expected from the fact that the optimal layout of an arch is dramatically different from the one of a beam shown in Section 3. Figure 16 shows the optimal distribution of stiffener or reinforcement layout of a shell for the case of a point transverse load applied at the center top of the shallow shell surface. A ring shape reinforcement is formed that is never be generated in a plate. Inner cross shape center stiffener in a plate disappear in a shell. Rather thick stiffeners are assigned along the diagonals. This is again, very different from the case of the plate. Hinges appears on the diagonal stiffeners, but they are different from the plate, too. Another difference is that scattered reinforcement is observed inside a ring stiffener when the volume of solid material for reinforcement is reduced. This indicates possibility of the microstructure of perforation over there. For the plate, all of stiffeners are solid.

Figure 17 shows the result of a shell for the distributed load. Basic pattern of distribution of stiffeners is similar to the one for the point load case, although they are more distributed in the four corners of a shell. Stiffeners in the center portion disappear in the distributed load case.

It is clear that very different layouts are obtained in a plate and a shell for the both loading cases. This difference may be explained by the fact that a shell is combination of a plate and a membrane. Quite large portion of applied forces is supported by membrane rather than plate in a shell structure. If pure flat plate is considered, all the loads must be supported as a plate. Thus, the mechanics nature of a shell is very different from that of a plate, and this difference implies different optimal layouts of reinforcement in design optimization.

6. Transition from a Plate to a Shallow Shell

As shown in above the layout for a shallow shell is different from the one for a plate. Thus, it may be interesting to investigate transition process from a shell to a plate by reducing the shell height z_{max} to zero. It is a natural question what happens in between. Does the basic pattern of the layout change suddenly at a certain point ? Figure 18 shows how the optimal distribution of reinforcement changes from Fig.14 (b) to Fig.17 (b). It is observed that sudden change does not occur, but changes are rather gradual. In other words, transition of the layout of a shell to that of a plate is "continuous." Since quantifying the change of topology is difficult, we shall display in Fig. 19 the change of the mean compliance in transition from a plate to a shallow shell. The uniformly distributed pressure is applied and the shape of the shell is the same to the one used in the previous section, while the shell height is varying from 0 to 4. Compliance change also shows very smooth transition from a plate to a shell, though there is a region in which compliance changes is very steep. It is natural to expect that in this region, the structure changes from "bending dominant" to "membrane dominant".

7. Optimum Layout of Reinforcement of a Folded Plate

We shall apply the homogenization method to find the optimum layout of a folded plate structure in order to demonstrate the capability of the present formulation for solving design problems in practice where many folded plates are used. Since this example is for showing the capability of the present formulation, we shall consider only a simple case as shown in Fig. 20 involving 90 degree folding. Three forces, F_x,

F_y, and F_z are separately applied to emphasize the special mechanics nature of the problem.

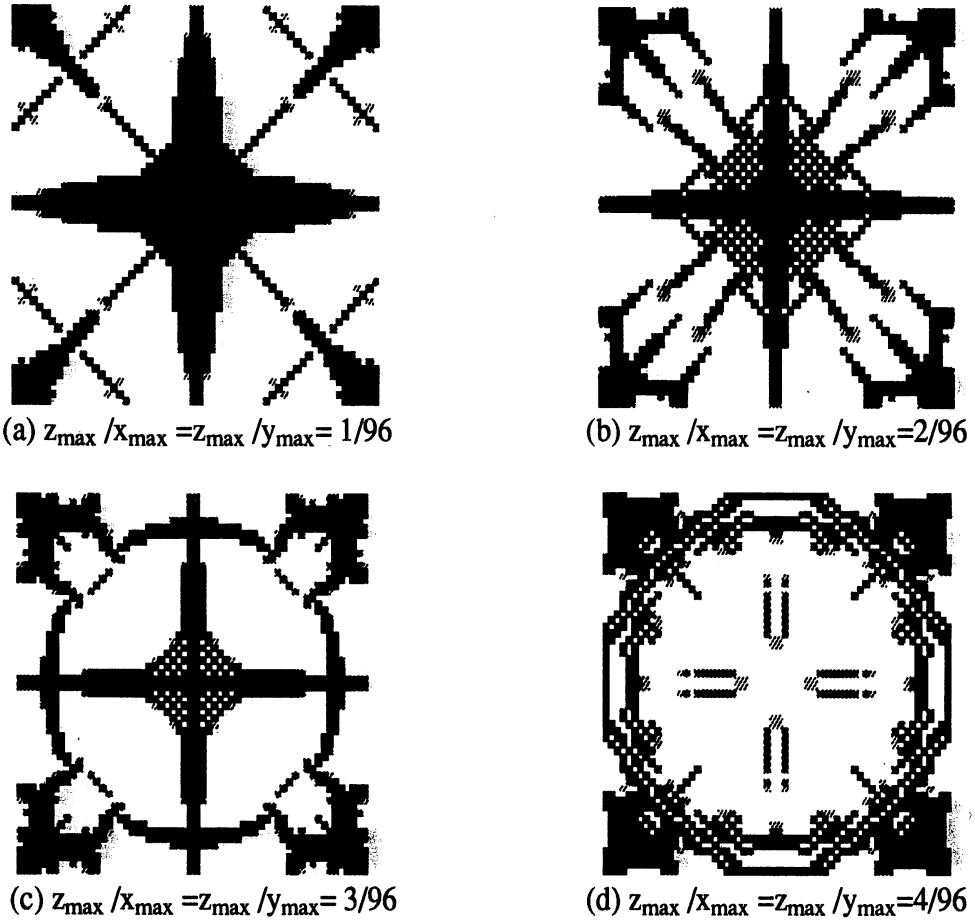

(a) $z_{max}/x_{max} = z_{max}/y_{max} = 1/96$ (b) $z_{max}/x_{max} = z_{max}/y_{max} = 2/96$

(c) $z_{max}/x_{max} = z_{max}/y_{max} = 3/96$ (d) $z_{max}/x_{max} = z_{max}/y_{max} = 4/96$

Figure 18 Optimal Reinforcement of Shells with Various Height
(Distributed Load, Volume 270/900)

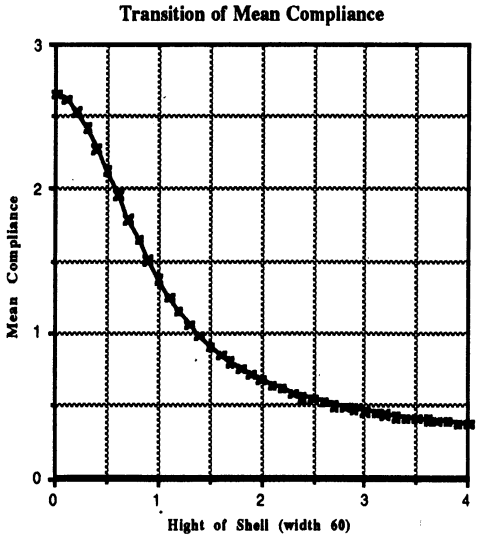

Figure 19 Change of the Mean Compliance

Force F_x provides transverse bending to both the standing and flat plates. Force F_y generates in plane bending to the standing plate while rather large torque is generated by this force in the lower flat plate. Force F_z gives just tension to the standing plate, and it provides both transverse bending and torsion to the lower flat plate. It is noted that effect of bending is much larger than torsion in this case.

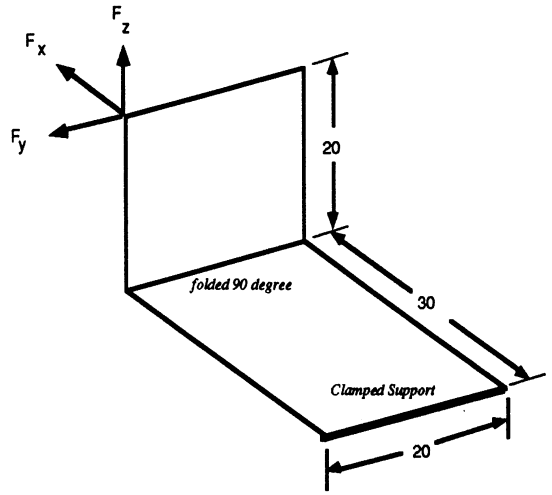

Figure 20 Design Domain of a Folded Plate and Three Different Loadings

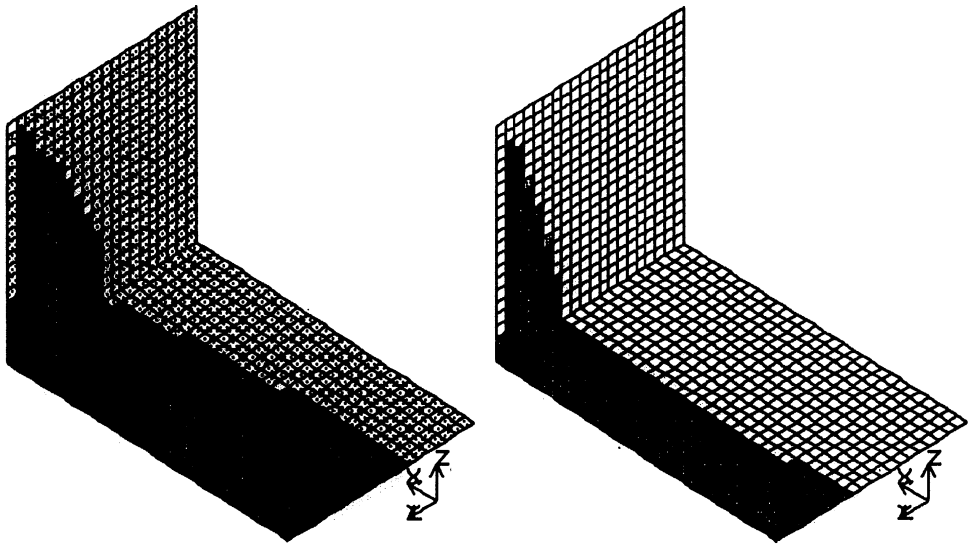

Figure 21 Optimum Layout of a Folded Plate for the Applied Load F_x

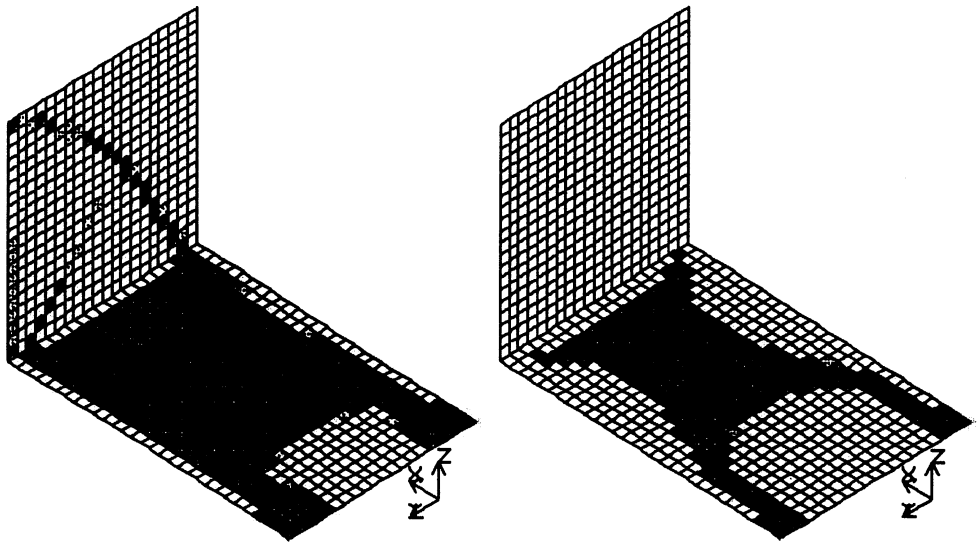

Figure 22 Optimum Layout of a Folded Plate for the Applied Load F_y

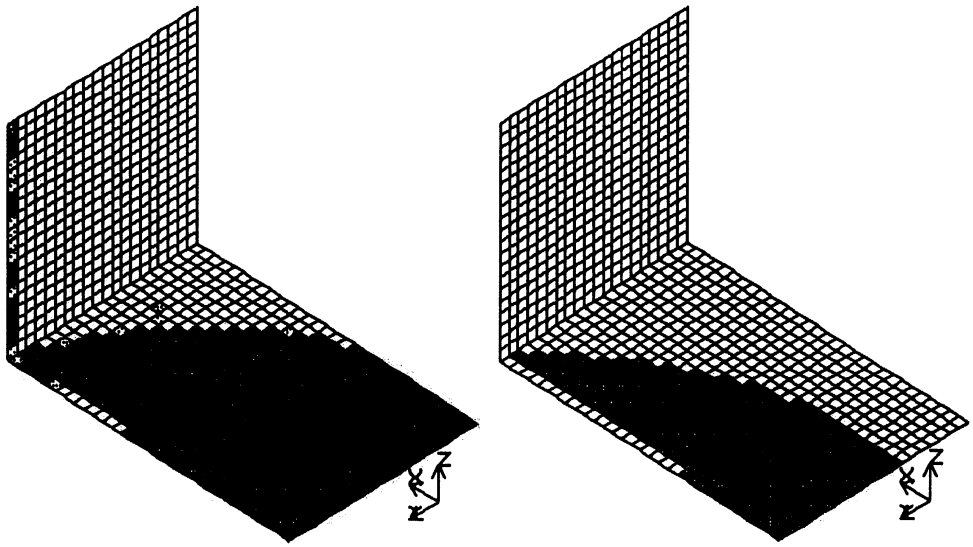

Figure 23 Optimum Layout of a Folded Plate for the Applied Load F_z

The standing plate is divided into 20 x 20 square uniform 4 node shell finite elements, while the lower flat plate is divided into 20 x 30 square uniform 4 node elements. This finite element model involves 6,426 degrees of freedom, and the total number of discrete design variables is 3,000. The thickness of the initial plate h_0 is assumed to be zero, and the height of "microscopic" stiffeners is assumed to be a constant, h_1=1 in the present example. Two different amounts of solid material are considered, say 500 and 300 for the total design domain that is expressed as 1,000 units. The optimum layouts of folded plates are described in Figs. 21, 22, and 23 for two different volume and for three different applied load at the upper-left corner of the standing plate.

When force F_x is applied to the folded plate, this generates basically transverse bending and rather small torsion. Since the height of the plate for layout is held to be

constant h_1=1 in this problem, the optimum layout obtained should be very similar to the one obtained by the width optimization of a beam subject to a transverse force applied at the free end of the cantilever. If force F_y is applied at the upper-left corner of the standing plate, in-plane bending moment is generated in the standing plate while large torque exists in the flat plate. Thus, a frame structure shown in Fig. 24 is formed in the standing plate portion.

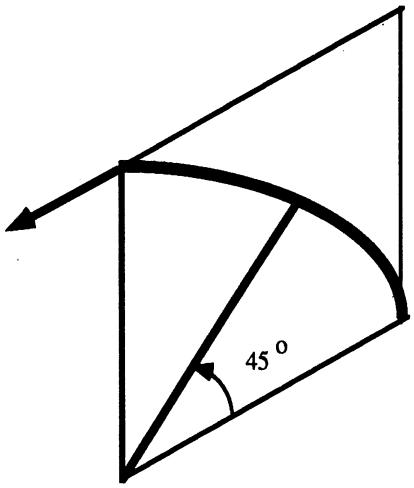

Figure 24 Frame Structure in the Standing Plate for In-Plane Bending

Since a downward force is applied at the left corner of the flat plate while a upward force is applied at the right corner, we have large torque in the flat plate portion, and then the layout is to resist to this torque. For force F_z, only tension force is generated in the standing plate, only a wire is need to sustain the tension in this portion. For the flat plate, bending and small torsion are applied, and the layout is very similar to the case of force F_x.

8. Optimum Layout of Reinforcement of a Shell Structure

As the last computational example, we shall obtain the optimum reinforcement of a cylindrical shell shown in Fig. 25. In this case, effect of the boundary condition on the optimum layout is examined. The height and the radius of the shell are h=20cm and r=20cm, respectively, and it is divided into 20x80 uniform size 4 node rectangular finite elements. A uniformly distributed moment is applied along the two vertical lines as shown in Fig. 25. Figure 26-(a) shows the layout of reinforcement when the both ends of the cylindrical shell is simply supported, while Fig. 26-(b) represents the optimum reinforcement when the both ends are free. Both cases tends to generates discrete ribs in the circumferential direction, although rather massive reinforcement is assigned along the lines on which the distributed moment is applied for the case of simply supported end condition.

9. Conclusions

The homogenization method to find the optimum layout of reinforcement of three-dimensional shell structures is presented in this article together with several

computational examples. As shown in above, without specifying the shape and topology of reinforcement of the shell initially built up, the optimum configuration can be obtained. The design variables are the size of rectangular parallelopipes in microscopic level as well as the rotation of these. Their height is held to be constant, while standard thickness optimization of a plate/shell utilizes the thickness as the design variable.

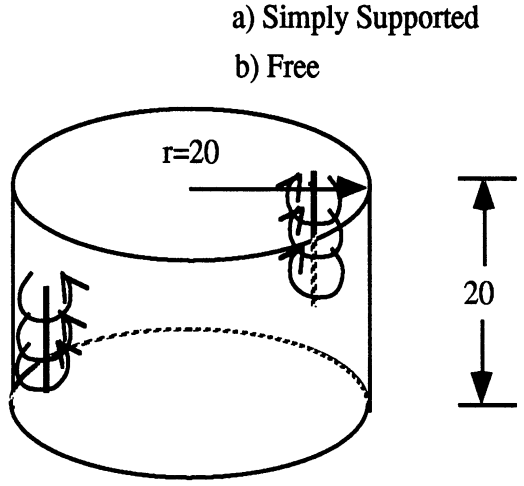

Figure 25 Cylindrical Shell with the Loading Condition

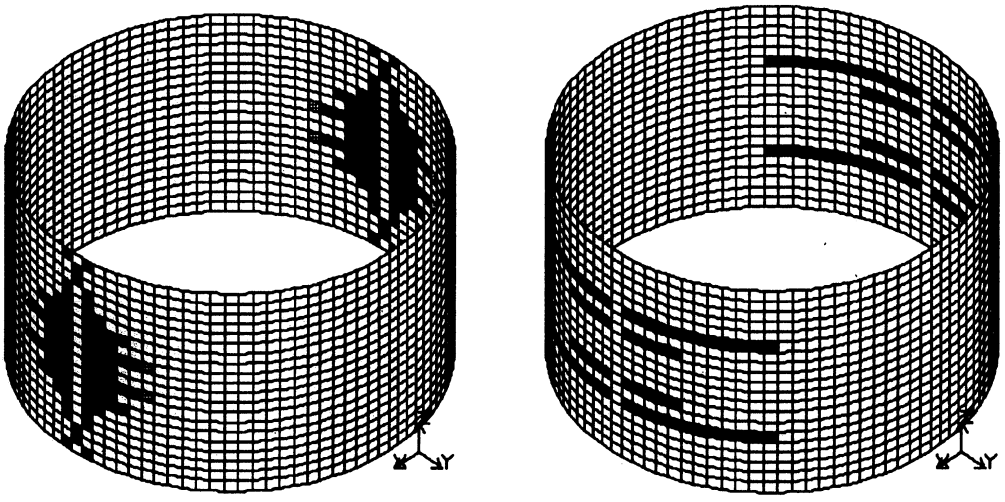

(a) Simply Supported (b) Free End Condition

Figure 26 Optimum Layout of Reinforcement of a Cylindrical Shell

The present formulation provides rather discrete solid stiffeners as the optimum reinforcement, and it generates very little portion of finely perforated reinforcement.

Convergence of finite element approximations is examined, and stable convergence is obtained for the example worked here. The present method is applied to obtain the optimum reinforcement for various cases of pates and shells in the three-dimensional space.

References

[1] Schmit, L.A., *Structural design by systematic synthesis*, Proceedings 2nd ASCE Conference on Electronic Computation (1960) pp.105-132, New York

[2] Fox, R. L., *Constraint surface normals for structural synthesis techniques*, AIAA J. 3-8 (1965) pp.1517-1518

[3] Prager, W and Taylor,J.E., *Problems of optimal structural design*, J. Appl. Mech. 35 (1968) pp.102-106

[4] Prager,W., *A note on discretized Michell structures*, Comput. Mechs. Appl. Mech. Engrg., 3-3 (1974) pp.349-355

[5] Michell, A.G.M., *The limits of economy of material in framed structures*, Phil. Mag. 6 (1904) pp.589-597

[6] Rozvany, G.I.N., *Optimal Design of Flexural Systems*, Pergamon Press, 1976, Oxford

[7] Bendsφe, M.P., and Kikuchi, N., *Generating optimal topologies in structural design using a homogenization method*, Comput. Meth. Appl. Mech. Engrg., 71 (1988) pp.197-224

[8] Suzuki K, Kikuchi N , *Homogenization Method for Shape and Topology Optimization*, Comp. Meth. Appl. Mech. Enginrg. to Appear in 1991

[9] Noor A.K., Belytschko, T., and Simo, J.C., *Analytical and Computational Models of Shells*, CED-Vol.3, American Society of Mechanical Engineers, (1989), New York

[10] Bendsφe, M.P., *Generalized Plate Models and Optimum Design*, in *Homogenization and Effective Moduli of Materials and Media*, ed. J.L. Ericksen et al., Springer-Verlag, (1986), New York, pp.1-26

[11] Schmit, L.A., Kicher, T.P., and Morrow, W.M., *Structural Synthesis capability for integrally stiffened waffle plates*, AIAA Journal, 1, (1963) pp.2820-2836

[12] Morrow, W.M., and Schmit, L.A., *Structural Synthesis of a Stiffened Cylinder*, NASA (1968) CR-1217

[13] Simitses, G.J., *Optimal versus the stiffened circular plate*, AIAA Journal, 11-10, (1973) pp.1409-1412

[14] Banichuk, N.V., *Problems and Methods of Optimal Structural Design*, Plenum Press, (1983), New York,

[15] Haftka, R.T., and Prasad, B., *Optimum structural design with plate bending elements - A Survey*, AIAA Journal, 19-4, (1981) pp.517-522

[16] Cheng, K.T., *On non-smoothness in optimal design of solid, elastic plates*, International Journal of Solids and Structures, 17, (1981) pp.795-810

[17] Cheng, K.T., and Olhoff N., *An investigation concerning optimal design of solid elastic plates*, International Journal of Solids and Structures, 17, (1981) pp.305-323

[18] Cheng, K.T., and Olhoff, N., *Regularized formulation for optimal design of axisymmetric plates*, International Journal of Solids and Structures, 18, (1982) pp.153-169

[19] Rozvany, G.I.N., *Structural Layout Theory - The Present State of Knowledge*, in *New Directions in Optimum Structural Design*, ed. E. Atrek et al, John Wiley & Sons, 1984, Chichester, pp.167-195

[20] Yang W.H., *Minimization Approach to Limit Solutions of Plate*, Comp Meth Appl Mech Enginrg 28 (1981) pp.265-274